JOURNAL OF MAGNETIC RESONANCE **135,** 298–309 (1998)
ARTICLE NO. MN981574

Symmetry and Phase-Selected NMR Spectra of Liquid Crystalline Samples

M. Carravetta,* F. Castiglione,*,† G. De Luca,* M. Edgar,* J. W. Emsley,*,[1] R. D. Farrant,‡ E. K. Foord,* J. C. Lindon,§ M. Longeri,† W. E. Palke,*,[2] and D. L. Turner*

*Department of Chemistry, University of Southampton, Southampton, SO17 1BJ, United Kingdom; †Dipartimento Di Chimica, Universita Della Calabria, 87030, Arcavacata Di Rende, Italy; ‡Physical Sciences, GlaxoWellcome Medicines Research Centre, Gunnels Wood Road, Stevenage, SG1 2NY, United Kingdom; and §Biological Chemistry, Division of Biomedical Sciences, Imperial College School of Medicine, London, SW7 2AZ, United Kingdom

Received May 1, 1998; revised July 30, 1998

It is demonstrated that the NMR spectra of liquid crystalline samples can be simplified by using multiple quantum filtering. In a system of N spin-$\frac{1}{2}$ nuclei, the N or (N-1)-multiple quantum filtered spectra (NQF or (N-1)QF) contain lines which originate only from transitions among the eigenstates belonging to the highest symmetry class of the spin permutation group. In addition the NQF spectra are divided further into two sets of lines which differ in phase by 180°. A method for simulating and analysing multiple quantum filtered spectra is described, with examples from molecules with up to eight interacting spins.

INTRODUCTION

The spectra of spin-$\frac{1}{2}$ nuclei in liquid crystalline samples are complex because they are dominated by the nuclear dipolar interaction. The anisotropic motion of the molecules in these samples leads to non-zero dipolar couplings, D_{ij}, between spins within the same molecule. The widths, Δ, of the lines is larger than in isotropic samples, but the ratio of Δ to the spectral width is similar to that in normal liquids, so that the spectra are well resolved, and can be classified as being of high resolution. The dipolar couplings between pairs of nuclei within a molecule are usually all large compared to the chemical shift, and so the spectra are very complex and can become very difficult to analyse as the number of interacting nuclei increases. Several methods have been proposed for aiding the analysis of these complex spectra. The most successful way of simplifying proton spectra is partial deuteriation, followed by deuterium decoupling (*1, 2*). However, the deuteriation may be difficult chemically, and is certainly tedious. Another approach is to obtain multiple quantum (ΔMQ) spectra as the F_1 projection in the 2D experiment illustrated in Fig. 1 (*3, 4*). For a set of N interacting spin-$\frac{1}{2}$ nuclei, the ΔMQ spectrum obtained for $\Delta M = \Delta\Sigma_i m_{zi} = N$ is a single line; m_{zi} is the magnetic quantum number for spin I. As ΔM decreases, the spectra increase in complexity, and it is often possible to extract all the dipolar couplings from the (N-1) and (N-2) MQ spectra. The signal-to-noise, S/N, ratio decreases rapidly as ΔM increases, and this, together with the 2D nature of the experiment means that the sensitivity per unit time is low, and is the limiting factor in the use of the multiple quantum spectra as the number of spins increases.

Another general way of aiding the analysis of complex spectra is to make use of any spin permutation symmetry present amongst the interacting spins. Thus the off-diagonal peaks ν_{ij} in a COSY spectrum will be present only if the diagonal peaks ν_i and ν_j arise from transitions between spin states belonging to the same symmetry class of the permutation group (*5–7*). This aids in the assignment of observed to calculated transition frequencies in the normal spectrum, and hence to the analysis of this spectrum by the standard, iterative procedures (*8, 9*). The large number of resolved transitions in the spectra of liquid crystalline samples requires high digital resolution in both dimensions of a COSY spectrum, which leads to very long recording times, and large data matrices. This has limited the application of COSY spectra of liquid crystalline samples to spin systems with no more than six interacting nuclei.

Avent (*10*) showed that liquid crystal spectra could be simplified by applying a multiple quantum filter if the spins have at least 2-fold permutation symmetry. The principle is that both the N and (N-1)Q coherences must belong to the highest symmetry class of the spin permutation group. The experiment is to create a pure NQ or (N-1)Q state, and then to convert this to single quantum coherence (1Q) which is detected as a 1D spectrum. This symmetry-filtered, (ΔMQF) spectrum contains lines originating only from the most symmetric class and hence contains substantially fewer lines than the non-filtered spectrum. The spectrometer available to Avent restricted his experiments to a four spin system. We describe here extensions of the ΔMQF experiment to larger numbers of interacting nuclei, and we show how these spectra can be analysed. We also show

[1] To whom correspondence should be addressed.
[2] On sabbatical leave. Permanent address: Department of Chemistry, University of California, Santa Barbara, CA 93106.

1090-7807/98 $25.00

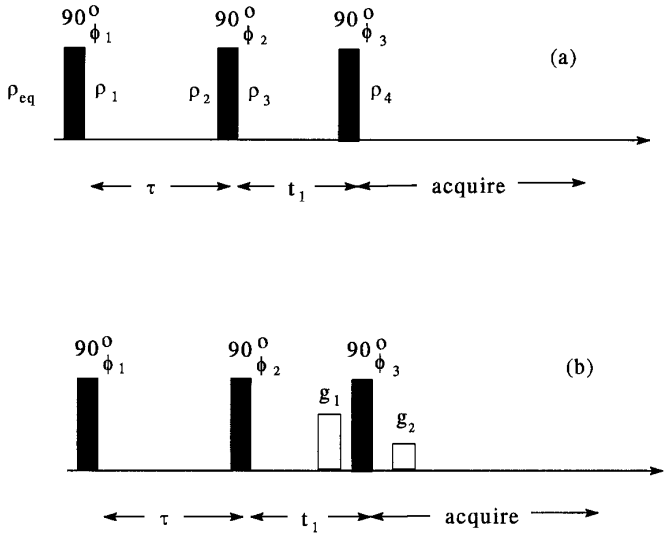

FIG. 1. Pulse sequences for generating multiple quantum filtered spectra (a) by cycling the phases ϕ_1, ϕ_2, and ϕ_3, and (b) by applying two field gradient pulses g_1 and g_2.

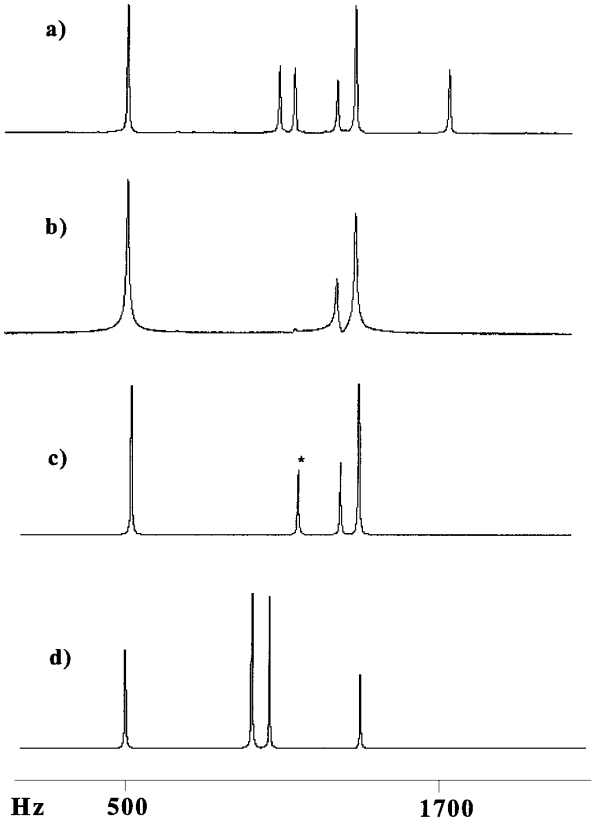

FIG. 2. The 600-MHz spectra of 1,2-dichlorobenzene dissolved in the nematic liquid crystalline solvent Phase 5 (Merck). Only the low frequency part of the spectrum is shown. (a) A non-filtered, 1Q spectrum. (b) A 3QF spectrum in magnitude mode. (c) A simulated 1Q spectrum but including only the symmetric transitions. Note that the transition marked * has a negligible experimental intensity. (d) A numerical simulation of a 3QF spectrum with the same parameters as in (c), except that the chemical shift difference is increased to 1600 Hz.

that the NQF spectra are sub-divided further on the basis of the relative phases of the lines.

EXPERIMENTAL

All orders of MQ coherences are generated by the two 90° pulses separated by an interval τ, as indicated in Fig. 1. The N or (N-1) MQ coherences may be selected either by phase cycling, as shown in Fig. 1a, or by the application of field gradient pulses, as shown in Fig. 1b (*4*). The selected MQ coherence is then converted to single quantum coherence by the third 90° pulse. In the 1D version of the experiment the delay t_1 shown in Fig. 1 is a fixed value, which is of sufficient duration to allow the phases or gradients to be switched. The experiment may also be performed as a 2D experiment, in which case the delay t_1 is incremented in the usual way.

The experiments using phase cycling were obtained using either a Bruker MSL 200 spectrometer or a Varian VXR 500. To select the coherences of order ΔM the phases $\phi_1 = \phi_2$ are advanced in 2ΔM successive experiments in steps of $2\pi/2\Delta$M, the third pulse has phase zero, and the receiver phase alternates between 0° and 180°. This results in the ΔMQF spectrum being the sum of coherence pathways involving both ΔM and $-\Delta$M. The experiment may also be done so as to select just one of these coherence transfer pathways, in which case the phases $\phi_1 = \phi_2$ are advanced in 4ΔM successive experiments in steps of $2\pi/4\Delta$M, and the receiver cycles through 0°, 270°, 180°, and 90°. This selects the $-\Delta$M pathway. The $+\Delta$M path can be selected with the same phase steps but the receiver phase is cycled through 0°, 90°, 180°, and 270°. The experiments using field gradients were acquired on a Bruker AMX-600 with an actively shielded *z*-gradient probe. The selection of the coherences depends on the relative areas of the two gradient pulses, and in this work the duration of both gradient pulses was fixed at 5 ms, and the relative amplitudes adjusted. The gradients

TABLE 1

Chemical Shifts, δ_i, and Dipolar Couplings, D_{ij}, Obtained by Analysing the 1Q 600-MHz Proton Spectrum of a Sample of 1,2-Dichlorobenzene Dissolved in the Nematic Solvent Phase 5

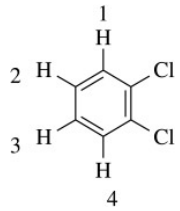

i,j	D_{ij}/Hz	J_{ij}/Hz[a]	δ_i/Hz
1,2	−906.6	8.0	0.0
1,3	−79.0	2.0	
1,4	−21.8	0.0	
2,3	−159.9	8.0	68.9

[a] Assumed and kept fixed in the iteration.

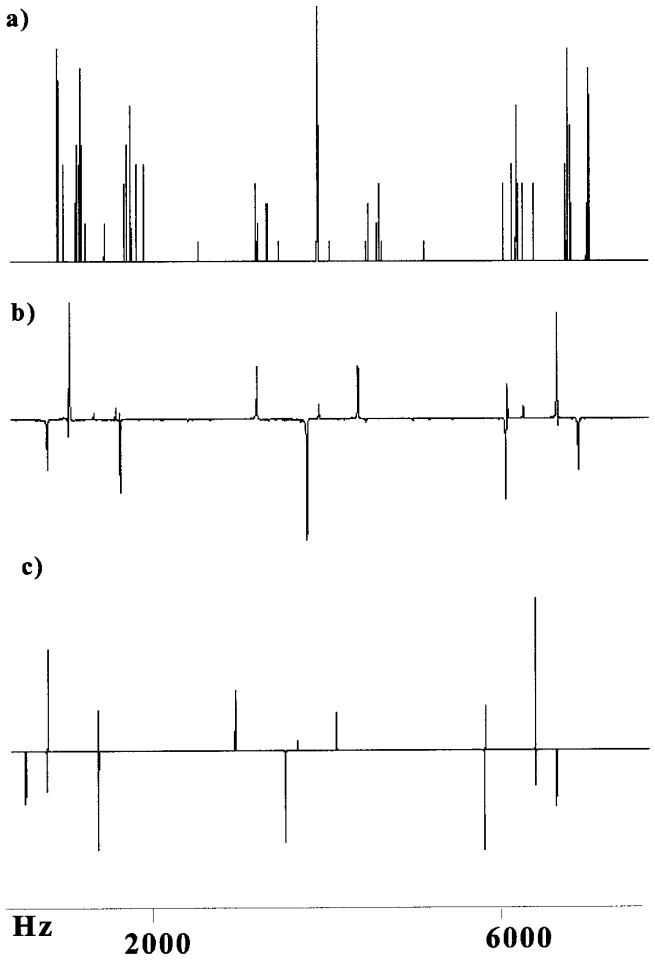

FIG. 3. (a) The 200-MHz ^{1}H 1Q spectrum of a sample of bromobenzene dissolved in the nematic solvent ZLI 1132 (Merck). (b) A 5QF spectrum obtained with a delay $\tau = 2.345$ ms, and with MQ selection achieved by phase cycling. (c) The 5QF spectrum calculated with parameters obtained from the iterative analysis of the experimental 5QF spectrum.

select just one coherence pathway, and so are equivalent to the phase cycling experiments with $4\Delta M$ steps. A comparison of the merits of the phase cycling compared to the field-gradient experiments is complicated by the large differences in the three spectrometers used. Suffice it to say that both experiments gave good results. The solutes were chosen to demonstrate particular spin systems, and they were dissolved in liquid crystalline solvents which were chosen to give well-resolved spectra at the probe ambient temperature.

ANALYSIS OF SYMMETRY SELECTED SPECTRA

The standard method for analysing ordinary NMR spectra is to simulate a spectrum by solving the time-independent Schrodinger equation

$$\mathcal{H}\psi_n = E_n\psi_n \qquad [1]$$

with a set of trial parameters. If the simulated and observed spectra are in close agreement it is possible to assign lines in the two spectra. The final stage is an iterative routine which brings the observed and calculated frequencies into best, least-squares agreement. Our original, rather simplistic approach was to analyse ΔMQF spectra by treating them as ordinary spectra, but arising only from the appropriate symmetry states, ψ_n^s. Thus, Eq. [1] is replaced with

$$\mathcal{H}\psi_n^s = E_n^s\psi_n^s. \qquad [2]$$

This certainly allows the frequencies in a ΔMQF spectrum to be simulated, but the intensities will not be correct if calculated as for a 1Q spectrum. The intensities are not used in the iterative steps, and so it might be thought acceptable to exclude their calculation from the analysis process. However, the intensities are used in the initial assignment step in the spectral analysis, and so some approximate calculation of their values is necessary. The situation is complicated further because the lines in a ΔMQF spectrum do not all have the same phase. One simple way of avoiding this

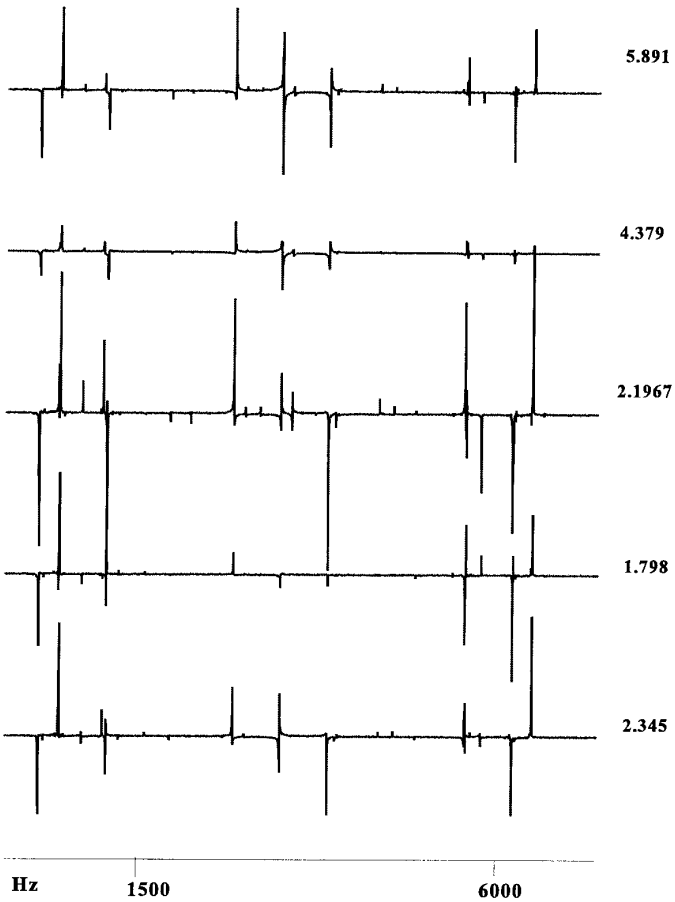

FIG. 4. The 200-MHz ^{1}H 4QF spectra of a sample of bromobenzene dissolved in the nematic solvent ZLI 1132 (Merck). The spectra are for the different values of the delay τ (ms) given alongside each spectrum.

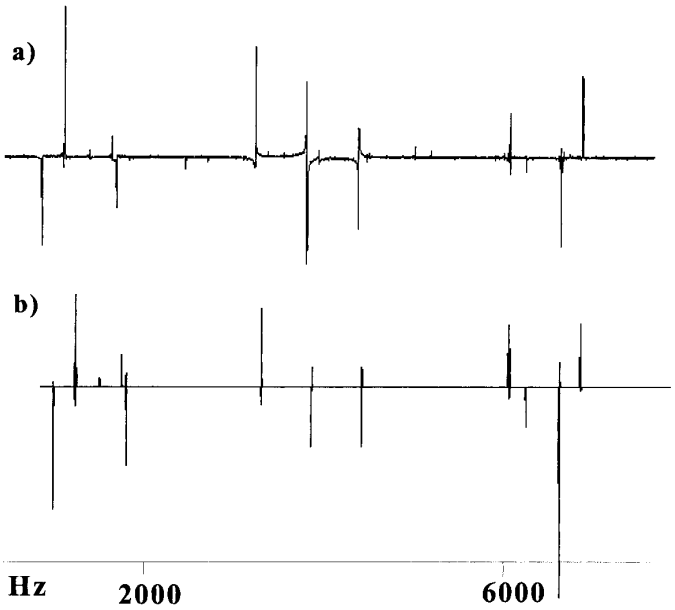

FIG. 5. The 200-MHz ^{1}H 4QF spectrum (a) of a sample of bromobenzene dissolved in the nematic solvent ZLI 1132 (Merck) obtained with a value of the delay $\tau = 5.891$ ms compared with (b) a spectrum simulated with the parameters obtained by iterative analysis.

complication is to calculate the magnitude spectrum. The simplistic approach, therefore, is to solve Eq. [2], to obtain the frequencies and intensities, and to compare these with an experimental magnitude spectrum.

However, this approach is flawed, because some of the expected signals may have vanishingly small intensity. To illustrate this point, we consider the ΔMQF magnitude spectrum given by the four protons in 1,2-dichlorobenzene (ODCB) dissolved in the liquid crystalline solvent Phase 5 (Merck), an AA′BB′ spin system, whose low frequency lines are shown in Fig. 2b. Analysis of the 1Q spectrum gave the parameters in Table 1, and these were used to simulate the 3QF spectrum shown in Fig. 2c by the simplistic approach. This clearly reveals that there is a line missing from the low frequency part of the experimental spectrum which appears in the simulated one with a large relative intensity, and there is a similar line missing from the high frequency group of lines (not shown here). The intensities in an NMR spectrum are proportional to $|\langle F_- \rangle|^2$, where $\langle F_- \rangle$ is the expectation value of the operator $F_- = F_x - iF_y$, where F_x and F_y are the operators representing the x and y components of the total nuclear spin angular momentum. The magnitude of $\langle F_- \rangle$ is given by

$$\langle F_- \rangle = \text{Trace}[\mathbf{F}_- \rho], \qquad [3]$$

where $\mathbf{F}_-$ is the matrix representing F_-, and ρ is the density matrix representing the state of the spin system immediately following the last pulse in the experimental sequence, both in the eigenbase, ψ_n, of the spin system. Thus, for an ordinary 1Q spectrum, ρ is that produced by the effect of a single $90°_x$ pulse on the initial, equilibrium state, and corresponds to ρ_1 in Fig. 1, while for a ΔMQF spectrum it is the result of the third pulse in the sequence given in Fig. 1, denoted by ρ_4. The elements of ρ_4 depend on the NMR parameters, but also on τ. However, changing τ for this sample gave ΔMQF spectra with essentially identical relative intensities, but whose absolute intensities vary in an oscillatory manner. A value for τ is chosen which gives the maximum absolute intensity for the ΔMQF spectrum.

The correct ΔMQF spectral intensities can be obtained from Eq. [3], but before discussing our analysis program which does this, it is instructive to explore further why the simple approach fails. That is, why the intensity of the line marked with an asterisk in Fig. 2c is practically zero. There would be fewer lines in a ΔMQF spectrum if the symmetry of the spin system was higher, so one possibility is that the protons in ODCB approximate to either an A_2B_2 or an AA′A″A‴. For an AA′BB′ to approximate an A_2B_2 system, $T_{AB'}$ must be similar to T_{AB}, where $T_{ij} = J_{ij} + 2D_{ij}$, and this is not true for ODCB. When

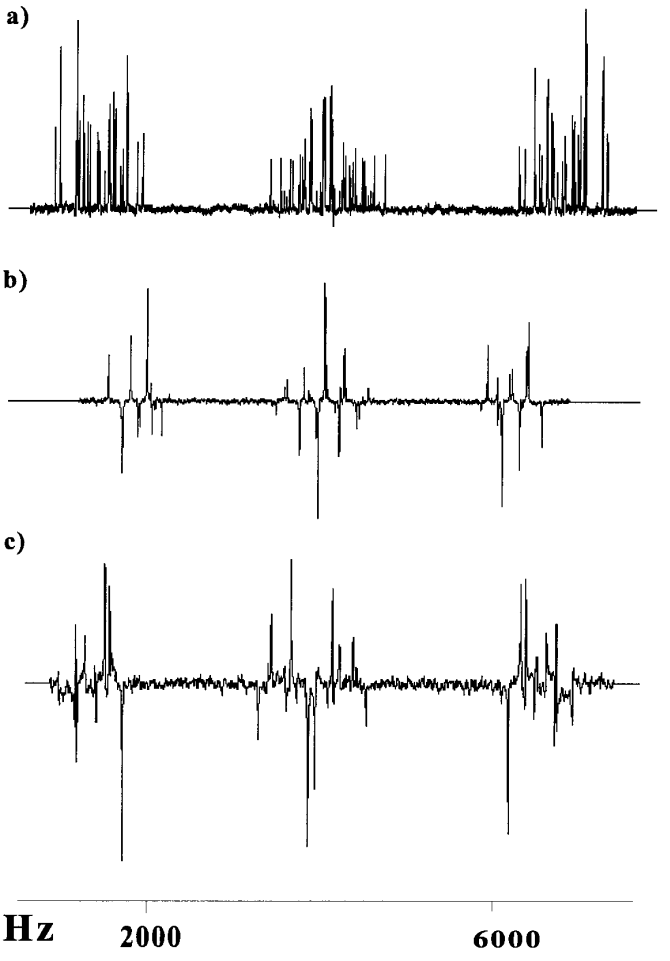

FIG. 6. The 200-MHz ^{1}H spectra of a sample of naphthaquinone dissolved in the nematic solvent ZLI 1132 (Merck). (a) The 1Q spectrum, (b) a 6QF spectrum with $\tau = 1.00$ ms, (c) a 5QF spectrum with $\tau = 3.33$ ms.

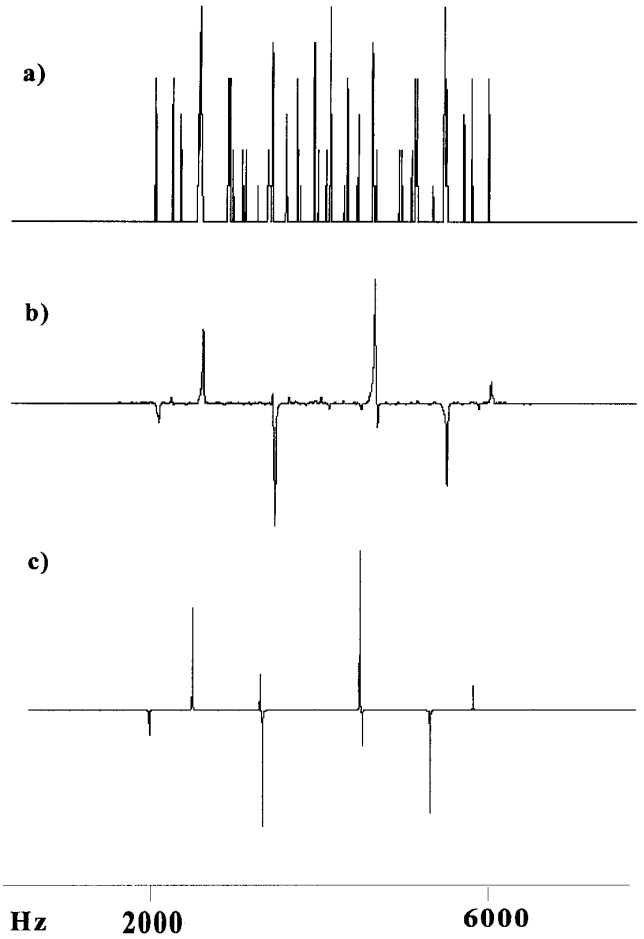

FIG. 7. The 188.3-MHz ^{19}F spectra of a sample of hexafluorobenzene dissolved in the nematic liquid crystalline solvent ZLI 1132. (a) A 1Q spectrum, (b) a 6QF observed with $\tau = 1.8$ ms, and (c) simulated from the parameters obtained by iterative analysis.

$\nu_A = \nu_B$, and $T_{AA'} = T_{BB'}$ and $T_{AB'} = T_{AB}$ the spin system becomes AA′A″A‴, but again this is far from being the case for ODCB as can be seen from the data in Table 1. The reason why the pair of lines are absent was discovered by first noting that these lines involve a spin state

$$\begin{aligned}\psi_{\text{abs}} = {} & 0.7067\alpha\alpha\beta\beta - 0.7036\beta\beta\alpha\alpha \\ & - 0.0529(\alpha\beta\alpha\beta + \beta\alpha\beta\alpha) \\ & - 0.0030(\alpha\alpha\beta\beta + \beta\beta\alpha\alpha) \qquad [4]\end{aligned}$$

which belongs to the symmetric $M = 0$ manifold, where $M = \Sigma_k m_k$ is the total magnetic quantum number of a spin state. This approximates to the function

$$\phi = 2^{-1/2}(\alpha\alpha\beta\beta - \beta\beta\alpha\alpha). \qquad [5]$$

We have, therefore, investigated using the following four symmetrised basis functions for deriving the symmetric $M = 0$ states of an oriented AA′BB′ spin system:

(1) $\chi_1 = 2^{-1/2}(\alpha\beta\alpha\beta + \beta\alpha\beta\alpha)$
(2) $\chi_2 = 2^{-1/2}(\alpha\beta\beta\alpha + \beta\alpha\alpha\beta)$
(3) $\chi_3 = 2^{-1/2}(\alpha\alpha\beta\beta + \beta\beta\alpha\alpha)$
(4) $\phi = 2^{-1/2}(\alpha\alpha\beta\beta - \beta\beta\alpha\alpha)$.

We then investigated the conditions in which ϕ is an eigenfunction of $\mathcal{H}$. This will be true if ϕ has zero off-diagonal hamiltonian matrix elements, H_{i4}, for $i = 1$, 2, and 3, or it will be an approximate eigenfunction if $(H_{i4}/H_{ii}) \ll 1$. The appropriate matrix elements are:

$$H_{14} = 0$$

$$H_{24} = 0$$

$$H_{34} = \nu_3 - \nu_1, \quad H_{33} = H_{44} = (T_{12} + T_{34})/2 - (T_{13} + T_{14})/4.$$

The function ϕ is an approximate eigenfunction, therefore, when the chemical shift difference is small compared with the total spin–spin couplings, and this is the case for the ODCB spectrum.

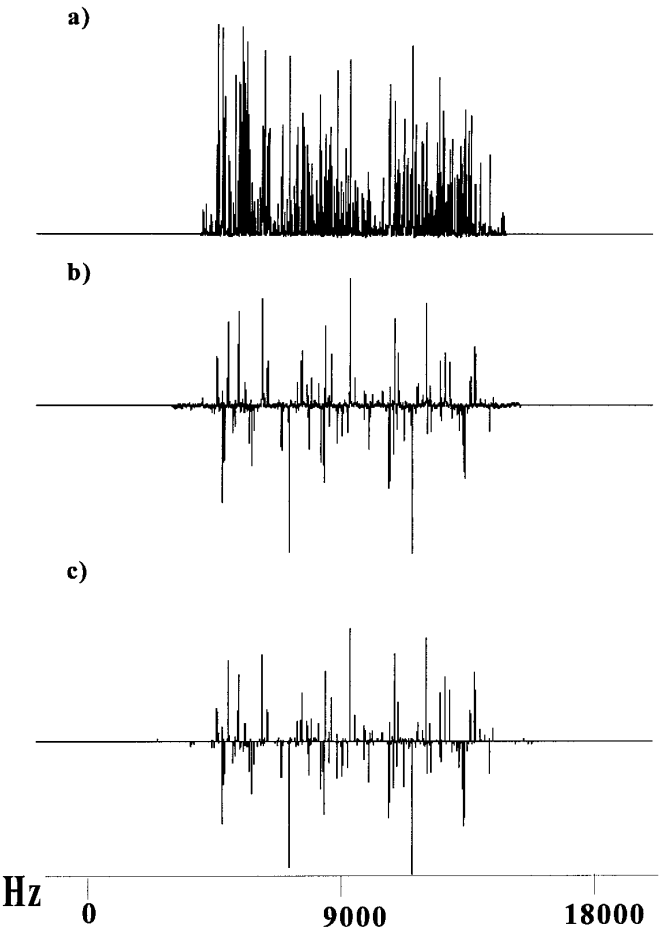

FIG. 8. (a) A 500-MHz ^{1}H spectrum of a sample of benzyl bromide dissolved in the nematic liquid crystalline solvent ZLI 1132. (b) The observed 7QF spectrum for $\tau = 1.3$ ms, compared with (c) the spectrum simulated with the parameters obtained by iterative analysis.

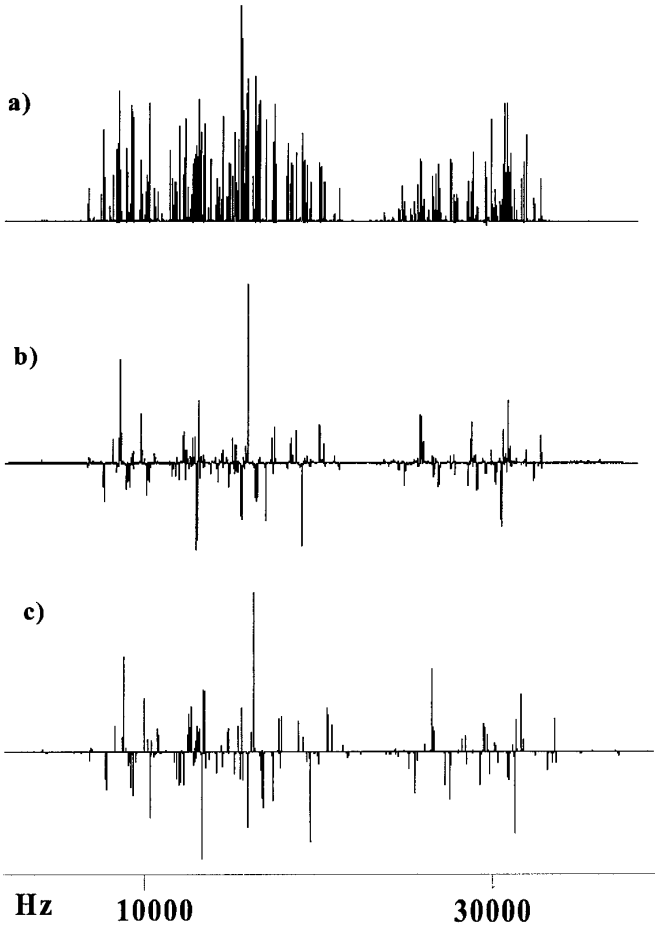

FIG. 9. (a) The 470-MHz ^{19}F spectrum of a sample of heptafluoropropyl iodide dissolved in the nematic liquid crystalline solvent ZLI 1132. (b) The 7QF spectrum obtained with $\tau = 2$ ms, compared with (c) the spectrum simulated with the parameters obtained from an iterative analysis.

This suggests that increasing the chemical shift for ODCB while keeping the couplings at their experimental values will lead to the appearance of all the symmetry-permitted lines in the ΔMQF spectrum. This is confirmed by a numerical simulation of the effect of the pulse sequence using a program developed by Palke *et al.* (*11*). The missing lines begin to appear when the chemical shift is 1600 Hz, as shown in Fig. 2d.

SIMULATION AND ITERATIVE ANALYSIS OF ΔMQF SPECTRA

The frequencies of the lines in an ΔMQF spectrum are obtained by solving Eq. [1], and the intensities from Eq. [3]. In fact, it is not necessary to select the solutions ψ_n^s from the more general states ψ_n in order to simulate a ΔMQF spectrum numerically, nor is it necessary to simulate the process by which the real experiments achieve ΔMQ selection, that is either phase cycling or field gradient pulses. The symmetry selection in the simulation is achieved simply by selecting the appropriate elements of ρ_3. We need consider only the effect of three pulses with a constant phase, for example, *x*. The general procedure adopted for calculating the values of the elements of the density matrices is based on that used by Palke *et al.* (*11*). The pulses are considered as instantaneous rotation operators, $\mathbf{R}_x(\pi/2)$ whose matrix elements, $R_x(\pi/2)_{jk}$ are evaluated in the product operator basis.

The spin system starts at thermal equilibrium, which has a diagonal density matrix, ρ^{eq} whose elements $\rho_{\ell\ell}^{eq}$ are the fractional populations of the spin states. The effect of the first pulse is to create ρ_1 with elements

$$\rho_{1jk} = \sum_\ell R_x(\pi/2)_{j\ell}\rho_{\ell\ell}^{eq}R_x(-\pi/2)_{\ell k}. \quad [6]$$

Free precession during τ produces ρ_2 with elements

$$\rho_{2jk} = \rho_{1jk}\exp(-i\omega_{jk}\tau), \quad [7]$$

where ω_{jk} is the frequency

$$\omega_{jk} = (E_j - E_k)2\pi/h \quad [8]$$

and the E_j are eigenvalues of the spin system.

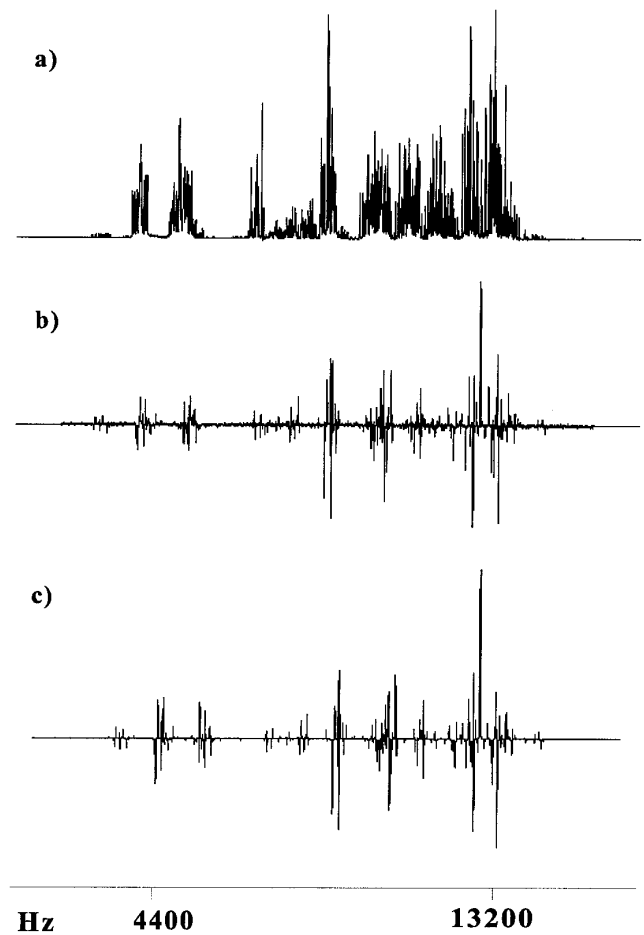

FIG. 10. (a) The 470-MHz ^{19}F spectrum of a sample of octafluoronaphthalene dissolved in the nematic liquid crystalline solvent ZLI 1132. (b) The 8QF spectrum obtained with $\tau = 6$ ms, compared with (c) the spectrum simulated with the parameters obtained from an iterative analysis.

TABLE 2

Chemical Shifts, δ_i, and Dipolar Couplings, D_{ij}, Obtained by Analysing the 1Q and 5QF 200-MHz Proton Spectra of a Sample of Bromobenzene Dissolved in the Nematic Solvent ZLI 1132

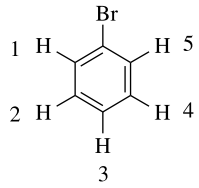

	D_{ij}/Hz			δ_i/Hz	
i,j	1Q	5QF	J_{ij}/Hz[a]	1Q	5QF
1,2	−1623.63 ± 0.05	−1624.9 ± 0.3	8.0	7.9 ± 0.3	8.0 ± 0.6
1,3	−237.2 ± 0.1	−237.3 ± 1.7	2.0		
1,4	−58.57 ± 0.04	−57.6 ± 2.8	0.0		
1,5	−14.0 ± 0.3	−14.6 ± 4.8	2.0		
2,3	−456.8 ± 0.1	−456.5 ± 1.0	8.0	0.0	0.0
2,4	−15.1 ± 0.3	−15.3 ± 1.9	2.0		
3				73.68 ± 0.08	74 ± 1

[a] Assumed and fixed in the iterations.

The second pulse generates ρ_3 whose elements are

$$\rho_{3mn} = \sum_{j,k} R_x(\pi/2)_{mj}\rho_{2jk}R_x(-\pi/2)_{kn}. \quad [9]$$

The period t_1 is typically 10 μs and in this short interval ρ_3 does not change, so that ρ_4 may be obtained as

$$\rho_{4pq} = \sum_{m,n} R_x(\pi/2)_{pm}\rho_{3mn}R_x(-\pi/2)_{nq}. \quad [10]$$

So far there is no multiple quantum, and hence symmetry, selection. To achieve this it is only necessary to select the appropriate elements from ρ_3. This is particularly simple if the

TABLE 3

Chemical Shifts, δ_i, and Dipolar Couplings, D_{ij}, Obtained by Analysing the 1Q and 6QF 200-MHz Proton Spectra of a Sample of Naphthaquinone Dissolved in the Nematic Solvent ZLI 1132

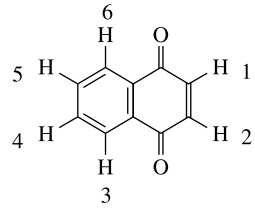

	D_{ij}/Hz			δ_i/Hz	
i,j	1Q	6QF	J_{ij}/Hz[a]	1Q	6QF
1,2	42.5 ± 0.1	42.9 ± 0.2	10.0		
1,3	−116.4 ± 0.3	−117.4 ± 0.8			
1,4	−96.1 ± 0.3	−94.9 ± 0.8			
1,5	−125.95 ± 0.07	−126.1 ± 0.1			
1,6	−346.89 ± 0.07	−347.1 ± 0.1	0.54		
3,4	−1937.61 ± 0.07	−1937.5 ± 0.2	7.81		
3,5	−124.14 ± 0.08	−124.2 ± 0.3	0.54		
3,6	3.1 ± 0.5	2.5 ± 1.0	0.54		
4,5	49.4 ± 0.5	50.8 ± 1.0	7.46		
1				47.9 ± 0.6	49.8 ± 1.2
3				71.6 ± 0.6	72.3 ± 1.2
4				0.0	0.0

[a] Assumed and kept fixed.

TABLE 4

Dipolar Couplings, D_{ij}, Obtained by Analysing the 1Q and 6QF 188.3-MHz Fluorine Spectra of a Sample of Hexafluorobenzene Dissolved in the Nematic Solvent ZLI 1132

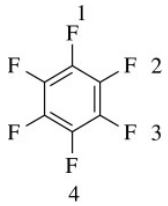

	D_{ij}/Hz		J_{ij}/Hz	
i,j	1Q	6QF	1Q	6QF
1,2	−572.58 ± 0.04	−572.0 ± 0.3	−22.4 ± 0.1	−23.1 ± 0.3
1,3	−107.07 ± 0.05	−106.0 ± 0.6	−3.5 ± 0.1	−2.8[a]
1,4	−76.42 ± 0.06	−75.8 ± 0.8	3.5 ± 0.2	3.8[a]

[a] Assumed from J. Gerritsen and C. McLean, *Rec. Trav. Chim.* **91,** 1393 (1972), and kept fixed.

NQ coherences are used to achieve the selection since these correspond to only the pair of elements ρ_{31L} and ρ_{3L1}, where $L = 2^N$ for spin $\frac{1}{2}$ nuclei, and more generally is the last row and column number in the matrix. All other elements ρ_{3pq} can be set to zero. Note that the two non-zero elements will be oscillating with time according to Eqs. [7] combined with [9], but for a particular value of τ they have a constant magnitude. The two elements are related by $\rho_{31L} = \rho^*_{3L1}$, where * denotes the complex conjugate. Thus the only computational steps required to obtain a NQF spectrum are the solution of eigenvalue equations for the spin system (remembering that symmetrised basis functions need not be used, but to do so will reduce the computational effort), the application of Eq. [10] with ρ_{3pq} containing $\rho_{31L} = \rho^*_{3L1}$ as the only non-zero elements, and then finally the application of Eq. [3] to evaluate the intensities. The element ρ_{31L} is in general a complex number $a + ib$, but in fact, as shown later, the action of the final pulse is to select either the real or imaginary part and so the NMR signals are proportional to either a or b depending upon whether N is odd or even.

To simulate a ΔMQF spectrum where the selection is via the (N-1) coherences requires the evaluation of the whole of ρ_3, but it is still not necessary to mimic the real experimental procedures for coherence selection. Selection is done simply by setting all elements in ρ_3 to zero except those corresponding to the (N-1) coherences. This means that to simulate an (N-1)QF spectrum is much more computationally demanding than an NQF, and this will be illustrated by particular examples. Note that the ΔMQF spectra are the same independently of whether both coherence pathways are selected by phase cycling, or just one, either by phase cycling or application of field gradients.

PHASE SELECTION

The NQF spectra have lines which differ in phase, but only by 180°, that is, the final spectrum can be phase corrected so

TABLE 5

Chemical Shifts, δ_i, and Dipolar Couplings, D_{ij}, Obtained by Analysing the 1Q and 7QF 500-MHz Proton Spectra of a Sample of Benzylbromide Dissolved in the Nematic Solvent ZLI 1132

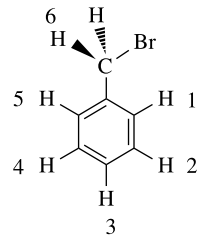

	D_{ij}/Hz			δ_i/Hz	
i,j	1Q	7QF	J_{ij}/Hz[a]	1Q	7QF
1,2	−1886.00 ± 0.07	−1886.0 ± 0.3	8	0.0	0.0
1,3	−266.5 ± 0.1	−265.9 ± 0.5	2		
1,4	−50.16 ± 0.07	−51.3 ± 0.5	0.5		
1,5	18.3 ± 0.2	19.3 ± 0.8	2		
1,6	−576.6 ± 0.1	−576.0 ± 0.4			
2,3	−390.05 ± 0.13	−390.4 ± 0.6	6	49.6 ± 0.2	49.3 ± 0.5
2,4	18.7 ± 0.19	19.9 ± 0.6	2		
2,6	−164.7 ± 0.1	−165.3 ± 0.4			
3,6	−127.93 ± 0.06	−127.1 ± 0.3		234.4 ± 0.1	234.3 ± 0.4
6,6	1362.05 ± 0.08	1362.9 ± 0.4		−743.49 ± 0.08	−743.4 ± 0.4

[a] Assumed and kept fixed.

TABLE 6

Chemical Shifts, δ_i, and Dipolar Couplings, D_{ij}, Obtained by Analysing the 1Q and 7QF 470-MHz Fluorine Spectra of a Sample of Heptafluoropropyl Iodide Dissolved in the Nematic Solvent ZLI 1132

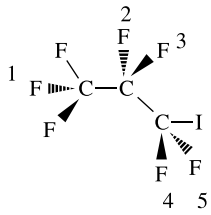

	D_{ij}/Hz		J_{ij}/Hz		δ_i/Hz	
i,j	1Q	7QF	1Q	7QF	1Q	7QF
1,1	1546.08 ± 0.06	1545.6 ± 0.2				
1,2	−663.29 ± 0.05	−663.3 ± 0.3	1.13[a]	1.13[a]		
1,4	−555.93 ± 0.06	−555.7 ± 0.2	9.24[a]	9.24[a]		
2,3	1678.0 ± 0.1	1682.6 ± 0.8	282.8 ± 0.4	266.9 ± 0.9		
2,4	394.5 ± 0.1	410.2 ± 1.6	3.66[a]	3.66[a]		
2,5	696.3 ± 0.1	682.8 ± 1.6	6.16[a]	6.14[a]		
4,5	1954.7 ± 0.1	1955.0 ± 0.4	222.7 ± 0.3	216.9 ± 0.9		
1					5176.0 ± 0.1	5173.1 ± 0.6
2					0.0	
4					−15630.3 ± 0.2	−15634 ± 1

[a] Taken from an analysis of an isotropic sample and kept fixed.

that lines have either phase 0° or 180°, and this is illustrated by the NQF spectra shown in Figs. 3–10. This phase selectivity can be exploited in the iterative spectral analysis, and makes NQF spectra even simpler than those which are only symmetry selected. Note that the phase selectivity is independent of whether a single pathway or both coherence pathways are selected in the experiment.

The phase selectivity can be understood by examining why a phase difference arises in these spectra. The lines in a ΔMQF spectrum are proportional to the single quantum coherences ρ_{4rs}, and these are characterised by a frequency, ω_{rs}, an amplitude, A_{rs}, and a phase, ϕ_{rs}. The ρ_{4rs} are generated by the action of the final 90° pulse from ρ_3, which for an N-selective scheme has non-zero elements ρ_{31L} and ρ_{3L1}. This means that the phases ϕ_{rs} are determined entirely by the action of the final 90° pulse, and not on the preceding part of the pulse sequence. The result of applying a rotation operator $R(\beta,\phi)$ for a pulse of general rotation angle β and phase ϕ to ρ_3 is given by (*12, 13*)

$$\rho_{4rs} = \sum_{tu} R_{rt}(\beta,\phi)\rho_{3tu}R_{us}^{-1}(\beta,\phi) \quad [11]$$

$$= \sum_{tu} Z_{rstu}(\beta,\phi)\rho_{3tu}, \quad [12]$$

where

$$Z_{rstu}(\beta,\phi) = R_{rt}(\beta,\phi)\,R_{us}^{-1}(\beta,\phi). \quad [13]$$

The change in phase and amplitude on transferring magnetisation from a coherence ρ_{3tu} to ρ_{4rs} is determined by $Z_{rstu}(\beta,\phi)$ which is

$$Z_{rstu}(\beta,\phi) = i^{(\Delta su-\Delta rt)}\sin(\beta/2)^{(\Delta su+\Delta rt)}\cos(\beta/2)^{(2N-\Delta rt-\Delta su)} \times \exp[-i\phi(M_r - M_t - M_u + M_s)]. \quad [14]$$

Here $M_r = \Sigma_k\, m_{kr}$ is the total magnetic quantum number of state r and Δrt is the number of spins which must be inverted to change state r into state t, so that

$$\Delta rt = \textstyle\sum_k |m_{kr} - m_{kt}|. \quad [15]$$

In the case of present interest $\beta = \pi/2$ and $\phi = 0$, and so

$$Z_{rstu}(\pi/2,\, 0) = i^{(\Delta su-\Delta rt)}(\tfrac{1}{2})^N. \quad [16]$$

To obtain the phases of the lines in a NQF spectrum we need consider only the case when the states t and u are the product functions $\Pi_k\alpha_k$, corresponding to $M_t = N/2$, and $\Pi_k\beta_k$, which has $M_u = -N/2$. A single quantum coherence, for which $M_r - M_s = -1$ will be between states with $M_r = -(N/2) + q$ and $M_s = -(N/2) + q + 1$, where $0 \le q \le N - 1$. The general value of Δsu is $N - q - 1$, while $\Delta rt = q$, which gives $\Delta su - \Delta rt = N - 2q - 1$. When N is even the factors $(\Delta su - \Delta rt)$ are odd numbers, and they are even numbers when N is odd.

When N is even the factors $i^{(\Delta su-\Delta rt)}$, which determine the phase, are either $+i$ or $-i$, which means that the relative

TABLE 7

Chemical Shifts, δ_i, and Dipolar Couplings, D_{ij}, Obtained by Analysing the 1Q and 8QF 470-MHz Fluorine Spectra of a Sample of Octafluoronaphthalene Dissolved in the Nematic Solvent ZLI 1132

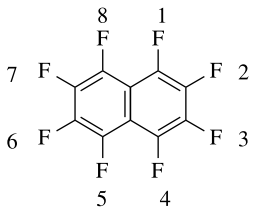

	D_{ij}/Hz		J_{ij}/Hz		δ_i/Hz	
i,j	1Q	8QF	1Q	8QF	1Q	8QF
1,2	−1213.9 ± 0.2	−1214.3 ± 0.1	−17.9 ± 0.3	−16.9[a]		
1,3	−73.5 ± 0.1	−72.7 ± 0.7	2.8[a]	2.8[a]		
1,4	−8.3 ± 0.1	−6.6 ± 0.1	16.0 ± 0.3	15.4[a]		
1,5	−28.93 ± 0.15	−30.72 ± 2.24	1.4[a]	1.4[a]		
1,6	−73.3 ± 0.1	−73.9 ± 0.7	−4.4[a]	−4.4[a]		
1,7	−228.3 ± 0.1	−227.5 ± 0.1	5.0[a]	5.0[a]		
1,8	−1796.2 ± 0.1	−1796.3 ± 0.1	58.9 ± 0.2	59.2[a]		
2,3	−8.2 ± 0.1	−7.8 ± 0.2	−19.4 ± 0.2	−17.9[a]		
2,6	−65.0 ± 0.1	−65.0 ± 0.3	8.8 ± 0.2	7.6[a]		
2,7	−85.36 ± 0.08	−84.8 ± 0.1	−2.9[a]	−2.9[a]		
1					0.0	0.0
2					3553.8 ± 0.1	3552.5 ± 0.2

[a] Taken from L. Cassidei, O. Sciacovelli, and L. Folani, *Spectrochim. Acta A* **38,** 755 (1982), and kept fixed.

phases of the lines in the NQF spectrum are either 0 or π. An odd value of N gives $i^{(\Delta su-\Delta rt)}$ as either $+1$ or -1, which again means that the relative phases of the lines in the NQF spectrum are either 0 or π.

The (N-1)Q selection does not produce a simple phase division. This is because there are 2N non-zero (N-1) coherences in ρ_3, and the last 90° pulse creates single quantum coherences from these in ρ_4 such that some elements will have both real and imaginary parts. The lineshapes in the (N-1)QF spectrum are therefore a linear combination of absorption and dispersion lineshapes.

EXAMPLES OF ANALYSING ΔMQF SPECTRA OF SPIN-$\frac{1}{2}$ NUCLEI

The simulation procedures have been incorporated into a 1Q simulation and iteration program, ARCANA (*14*). We have chosen spin systems of increasing complexity to illustrate the simplifications which can be achieved by recording ΔMQF rather than normal 1Q spectra.

Bromobenzene

Figure 3 shows the 1Q proton spectrum of a sample of bromobenzene dissolved in the liquid crystal solvent ZLI 1132, an example of an AA′BB′C spin system. Figure 3 also shows a 5QF spectrum obtained by phase cycling. The absolute, but not the relative intensities depend on τ, but it is a simple task to do preliminary experiments to obtain a value which gives a good signal-to-noise ratio. The separation by phase is now such that each sub-spectrum contains a sufficient number of lines and can be analysed separately to yield the parameters. However, it is always better to use as many lines as possible in an analysis, and so it is preferable to use lines of both phases together. The advantage of the phase separation is in the crucial step of assigning calculated to observed lines. Table 2 shows the result of analysing the 5QF spectrum, compared with the data obtained by analysis of the normal, non-selected spectrum.

A series of 4QF spectra corresponding to different values of τ are shown in Fig. 4. It is apparent that the relative intensities depend on τ, and that some of the spectra contain more lines than the 5QF spectrum. This is an advantage in the analysis, but it is offset by the disadvantage of an increase in the time taken to simulate a (N-1)QF spectrum. The lines have phases between 0° and 180°, and these can be calculated as shown in Fig. 5, which compares a simulated with an observed 4QF spectrum. The phase dispersion is again useful at the assignment stage in the spectral analysis.

Naphthaquinone

This is an example of an AA′BB′CC′ spin system. Figure 6 shows the 1Q, 6QF, and 5QF spectra; the ΔMQF spectra were obtained with a value of τ which gives a good S/N, and for the 5QF spectrum, the largest number of strong lines. Again there is a phase selection for the 6QF spectra, but not for 5QF. The

5QF spectrum has an appreciably better S/N for the same number of transients, but this advantage is more than offset by the disadvantage of the increased computer time required to analyse a (N-1)QF spectrum. Table 3 compares the results from analysing the 1Q and the 6QF spectra.

Hexafluorobenzene

Figure 7 shows 1Q and 6QF spectra of a sample dissolved in ZLI 1132. The spin system is an AA′A″A‴A⁗ A⁗′. The 6QF spectrum, when compared with those from the six spin system of naphthaquinone, demonstrates that the simplification achieved by the symmetry selection increases as the symmetry increases. There are 72 lines in the 1Q spectrum, while only 8 strong lines can be seen in the 6QF, and these are equally divided into the phase sub-spectra. This reduced number of lines is still sufficient to obtain the three dipolar couplings, but not the three scalar couplings. Table 4 gives the parameters obtained from analysing these spectra.

Benzyl Bromide

Figure 8 shows the 500-MHz 1Q and 7QF spectra of a sample dissolved in ZLI 1132. Analysis of the AA′BB′CD_2 1Q spectrum had been achieved previously by synthesis of partially deuteriated samples and deuterium decoupling. It was used here to demonstrate the simplification achieved for such a spin system, and to show that the symmetry and phase selected spectra can be analysed to yield parameters in good agreement with those obtained from the 1Q spectrum, as shown in Table 5.

Heptafluoropropyliodide

The 1Q 470-MHz ^{19}F spectrum of a sample dissolved in ZLI 1132 is shown in Fig. 9, where it is compared with the 7QF spectrum. This is an example of a complex 1Q spectrum whose analysis was achieved by using a ΔMQF spectrum, and without having prior knowledge of good starting values for the parameters. A number of trial simulations were made using dipolar couplings, D_{ij}, estimated by assuming that the molecule is in a single fixed conformation with the iodine and the CF_3 group *trans* to one another. The spins form an AA′BB'_3C system, and one point of interest is that the 1Q spectrum of an isotropic solution has $|J_{AB} + J_{AB'}| \ll |J_{AA'} + J_{BB'}|$, and this means that the spectrum is deceptively simple and cannot be used to obtain $J_{AA'}$ or $J_{BB'}$. The spectrum of the liquid crystalline solution is sensitive to the magnitude of $|T_{AB} + T_{AB'}|$ relative to $|T_{AA'} + T_{BB'}|$ and is no longer deceptively simple; T_{ij} is the total spin–spin coupling and is given by

$$T_{ij} = J_{ij} + 2D'_{ij},$$

where D'_{ij} is the total anisotropic spin–spin coupling. D'_{ij} and D_{ij} are related by

$$D'_{ij} = D_{ij} + J_{ij}^{\text{aniso}},$$

where J_{ij}^{aniso} is the anisotropic contribution to the electron mediated spin–spin coupling. The parameters obtained by analysis of the 1Q and 7QF spectra are given in Table 6.

Octafluoronaphthalene

Figure 10 shows the 1Q, and the 8QF 470-MHz ^{19}F spectra of this AA′ A″ A‴BB′B″B‴ spin system. The symmetry and phase selection produces a large spectra simplification, thus there are 2860 transitions in the 1Q, and 940 in the 8QF spectra. The analysis proceeded by simulating a 8QF spectrum using dipolar couplings similar to inter-proton couplings found for a sample of naphthalene dissolved in a liquid crystalline solvent. The phase separation was found to be very useful in the assignment of calculated to observed lines; 135 lines could be assigned. Having analysed the 8QF spectrum it was possible to use the parameters to simulate a 1Q spectrum in very good agreement with that observed, and to assign 520 lines. The results of the analysis are shown in Table 7. The values of the J_{ij} were taken from an analysis of the spectrum of an isotropic sample, and then the larger values were allowed to vary in the iteration.

CONCLUSIONS

It is demonstrated here that it is possible to obtain good quality ΔMQF spectra of spin-$\frac{1}{2}$ systems containing as many as eight interacting nuclei. In the case of NQF spectra, these are divided into two sub-spectra which differ by a 180° phase shift. The simulation of NQF spectra is only a little more demanding of computer resources than are 1Q spectra, and an algorithm has been developed which allows them to be analysed by an iterative procedure which is similar to that used for 1Q spectra. The NQF spectra are easier to assign than 1Q spectra, and since this is the crucial step in spectral analysis, it means that there is a considerable advantage in recording and analysing a NQF spectrum prior to analysing the 1Q spectrum. Calculation of (N-1)QF spectra is more time-consuming, but these too can be useful at the assignment stage in a spectral analysis.

ACKNOWLEDGMENT

This work was supported by the Engineering and Physical Sciences Research Council.

REFERENCES

1. J. W. Emsley, J. C. Lindon, J. M. Tabony, and T. H. Wilmshurst, *J. Chem. Soc. Chem. Commun.* 1277 (1971).
2. S. Meiboom and L. C. Snyder, *Acc. Chem. Res.* **4,** 81 (1971).
3. A. Pines, D. Wemmer, J. Tang, and S. W. Sinton, *Bull. Am. Phys. Soc.* **23,** 21 (1978).
4. L. D. Field, *in* "Encyclopedia of NMR" (D. M. Grant and R. K. Harris, Eds.), p. 3172, Wiley, Chichester (1996).

5. M. Albert Thomas, K. V. Ramanathan, and A. Kumar, *J. Magn. Reson.* **55,** 386 (1983).
6. K. Rukmani and A. Kumar, *Chem. Phys. Lett.* **133,** 485 (1987).
7. P. Pfändler and G. Bodenhausen, *J. Magn. Reson.* **91,** 65 (1991).
8. S. Castellano and A. A. Bothner-By, *J. Chem. Phys.* **41,** 3863 (1964).
9. M. Longeri and G. Celebre, *in* "Encyclopedia of NMR" (D. M. Grant and R. K. Harris, Eds.), p. 2774, Wiley, Chichester (1996).
10. A. G. Avent, *J. Magn. Reson.* **53,** 513 (1983).
11. W. E. Palke, J. T. Gerig, and S. L. Smith. Program available from the authors, Department of Chemistry, University of California, Santa Barbara, CA 93106.
12. L. Braunschweiler, G. Bodenhausen, and R. R. Ernst, *Mol. Phys.* **48,** 535 (1983).
13. D. L. Turner, *J. Magn. Reson.* **46,** 213 (1982).
14. G. Celebre, G. De Luca, M. Longeri, and E. Sicilia, *J. Chem. Inf. Comput. Sci.* **34,** 539 (1994).